Journal of Engineering Mathematics **39:** 241–259, 2001.

Analytical approximations to the viscous glass-flow problem in the mould-plunger pressing process, including an investigation of boundary conditions

S.W. RIENSTRA and T.D. CHANDRA[1]
Department of Applied Mathematics and Computing Science, Eindhoven University of Technology, P.O. Box 513, 5600 MB Eindhoven, The Netherlands
[1]*Department of Mathematics of State University of MALANG, Malang, Indonesia*

Received 10 February 2000; accepted in revised form 15 September 2000

Abstract. Industrial glass is produced at temperatures above 600 °C, where glass becomes a highly viscous incompressible fluid, usually considered as Newtonian. In the production two phases may be distinguished, namely the pressing phase and the blowing phase. This study will be concerned with glass flow in the pressing phase, which is called thus because a blob of fluid glass (called a gob) is pressed in a mould by a plunger, such that the glass flows between mould and plunger, in order to obtain the preform of a bottle or jar, called a parison. In the blowing phase (not considered here) the parison is subsequently blown into the final shape of the product. By application of the slender geometry of mould and plunger and a cylindrical symmetry, a form of Reynolds's lubrication flow equations is obtained. These equations are solved by utilizing the incompressibility of the glass, by which the flux at any axial cross section is determined for prescribed plunger velocity, leading to analytical results in closed form for velocity field and pressure gradient. The glass level is implicitly defined by the integral over the varying volume which is to remain constant. The pressure may then be determined by integration. Special attention is given to the required boundary conditions. It is known that, depending on several problem parameters like temperature, pressure, and smoothness of the wall, the glass flow slips, to some extent, along the wall. Therefore, this study includes a general formulation of the boundary condition of partial slip in the form of a linear relation between shear stress and slip velocity, also known as Navier's slip condition. The coefficient of this relation, a positive number, may vary in our solution with axial position, but depends on the problem and is to be obtained from (for example) experiment. Two special cases, which seem to be relevant in practice, are considered as examples: (i) no slip on both plunger and mould; (ii) no slip on the mould and full slip (zero friction) on the plunger. The results are compared with fully numerical (FEM) solutions of a Stokes-flow model, and the agreement is good or excellent. Since in any practical situation it is not the plunger velocity which is prescribed, but (within practical limits) the force applied by the plunger, the problem of a prescribed plunger force has also been investigated.

Key words: glass, viscous flow, slender geometry, slip and no-slip boundary conditions, lubrication theory.

1. Introduction

Glass is a widely used packing material, for example in the form of jars and bottles in the food industry. The production of glass forms like jars proceeds more or less along the following lines [1, pp.612–613]. First, grains and additives, like soda, are heated in a tank. Here gas burners or electric heaters provide the heat necessary to warm the material up to some 1200 °C. At one end the liquid glass comes out and is led to a pressing or blowing machine. To obtain a glass form, a two-stage process is often used. First (Figure 1), a blob of hot glass called a gob falls into a configuration consisting of a *mould* and *plunger*. As soon as the entire glass drop has fallen into this mould, the plunger starts moving to press the glass. This process is

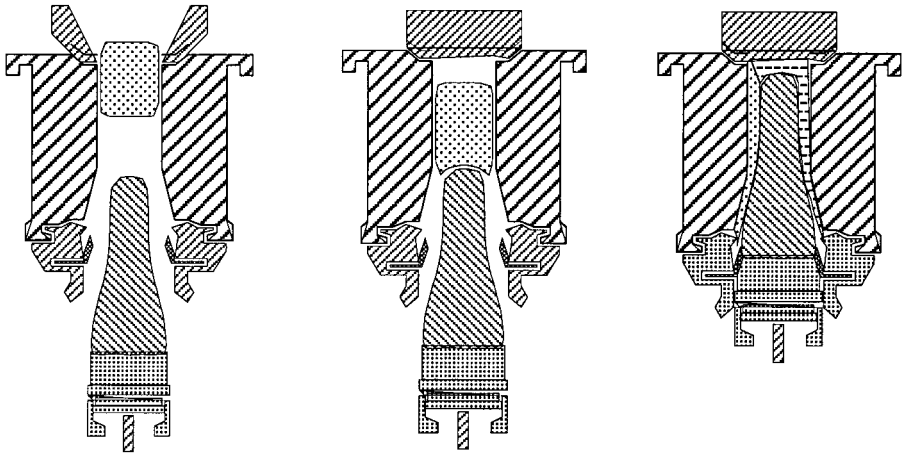

Figure 1. Pressing phase

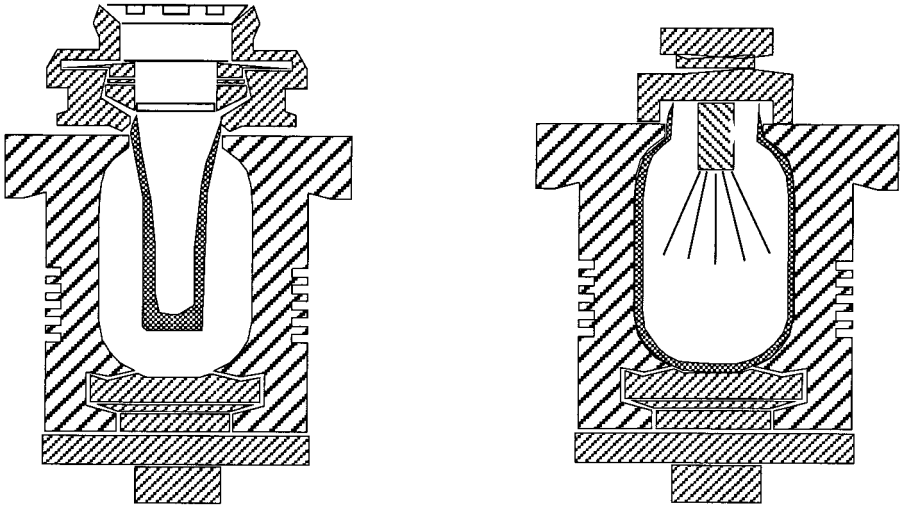

Figure 2. Blowing phase

called *pressing*. At the end, the glass drop is reshaped into a preform of a bottle or jar, called a *parison*. After a short period of time, for cooling purposes (the mould is kept at 500 °C) , the parison is blown to its final shape in another mould. This process is called *blowing* (see Figure 2).

The contents of this paper concern glass flow in the pressing phase in manufacturing glass jars or parisons. A typical feature of the shape of a parison is that wall thickness and radius vary very slowly (except for the bottom part), see Figure 3. In the present paper, this slow variation will be utilized to obtain an explicit, analytical description of velocity and pressure gradient of the glass flow.

2. Governing equations

The motion of glass at temperatures above 600°C can be described by the Navier-Stokes equations for incompressible Newtonian fluids [2, p.3], given by

$$\rho\Big(\frac{\partial \boldsymbol{v}}{\partial t} + \boldsymbol{v}\cdot\nabla\boldsymbol{v}\Big) = \nabla\cdot\boldsymbol{\sigma}, \qquad \nabla\cdot\boldsymbol{v} = 0, \tag{1a, b}$$

where $\boldsymbol{v}$ denotes the velocity field, and ρ the density. Further, $\boldsymbol{\sigma}$ is the fluid stress tensor

$$\boldsymbol{\sigma} = -p\,\boldsymbol{I} + \boldsymbol{\tau}, \quad \text{or} \quad \sigma_{ij} = -p\,\delta_{ij} + \tau_{ij}, \tag{2}$$

where p is the pressure, $\boldsymbol{I} = (\delta_{ij})$ is the unit tensor, defined by $\delta_{ij} = 1$ if $i = j$, and $= 0$ otherwise, and $\boldsymbol{\tau}$ is the deviatoric or viscous stress tensor. In Newtonian fluids, a linear relationship is assumed between $\boldsymbol{\tau}$ and the deformation rate of the fluid element, expressed in the rate-of-strain tensor $\dot{\boldsymbol{\gamma}} = \nabla\boldsymbol{v} + (\nabla\boldsymbol{v})^{\mathrm{T}}$:

$$\boldsymbol{\tau} = \eta\,\dot{\boldsymbol{\gamma}} \quad \text{or} \quad \tau_{ij} = \eta\left(\frac{\partial v_i}{\partial x_j} + \frac{\partial v_j}{\partial x_i}\right), \tag{3}$$

where η is the dynamic viscosity. In general η depends on temperature, and may vary in space and time, but for a uniform temperature as we have here (approximately; see Section 4), η remains constant. Together with $\nabla\cdot\boldsymbol{v} = 0$, $\nabla\cdot\boldsymbol{\sigma}$ reduces to $-\nabla p + \eta\nabla^2\boldsymbol{v}$. As a result, Equations (1*a*,*b*) assume their common form

$$\rho\Big(\frac{\partial \boldsymbol{v}}{\partial t} + \boldsymbol{v}\cdot\nabla\boldsymbol{v}\Big) = -\nabla p + \eta\nabla^2\boldsymbol{v}, \qquad \nabla\cdot\boldsymbol{v} = 0. \tag{4a, b}$$

In view of the geometry of plunger and mould, we choose cylindrical coordinates (r, θ, z), and v, w, u will denote the r, θ, z components of the velocity $\boldsymbol{v}$. We assume the problem to be axisymmetric, so that both w and all θ-derivatives vanish, and the problem reduces to a two-dimensional one in the (r, z)-plane (see Figure 3).

3. Slender-geometry approximation

We will concentrate our analysis on the flow in the narrow annular duct between plunger and mould ($z > z_p$, see Figure 3). This region is very slender, and therefore amenable to asymptotic analysis [3, p.182], while at the same time the flow in the region between mould bottom and plunger top is practically stagnant, and therefore less important.

We will make Equations (4*a*,*b*) dimensionless by a suitable scaling. From the geometry of plunger and mould, we have two relevant length scales, the wall thickness of the parison, D, and the length of the plunger, L, while $D \ll L$. Except right near the plunger top, any variation in z scales on L and any variation in r scales on D. Therefore, we scale z with L and r with D, while we introduce the small parameter

$$\varepsilon = \frac{D}{L}. \tag{5}$$

The axial velocity u scales on a typical velocity V, while from the equation of mass conservation it follows that the radial velocity v has to scale on εV. As density ρ and viscosity η are

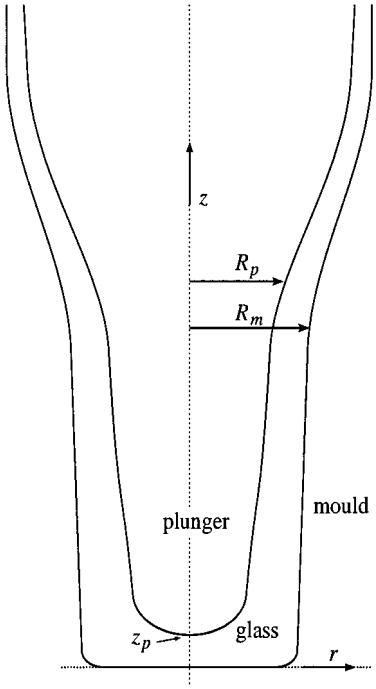

Figure 3. Sketch of configuration. Note that $R_p = R_p(z - z_p)$ is the surface of the plunger, $R_m = R_m(z)$ is the surface of the mould and z_p is position of the top of the plunger.

constant, they are parameters of the problem. Pressure p is to be scaled on $\eta VL/D^2$ (rather than ρV^2), because the glass flow is highly viscous, as we will see below. We have then

$$z = Lz^*, \quad r = Dr^*, \quad u = Vu^*, \quad v = \varepsilon Vv^*, \quad p = \frac{\eta VL}{D^2}p^*, \quad t = \frac{L}{V}t^*.$$

Now we substitute the above scalings in the Navier-Stokes equations and henceforth ignore the asterisks *, to obtain, respectively, the dimensionless z, r-components of the Navier-Stokes equations and the continuity equation, *viz.*

$$\varepsilon \mathrm{Re}\Big(\frac{\partial u}{\partial t} + u\frac{\partial u}{\partial z} + v\frac{\partial u}{\partial r}\Big) = -\frac{\partial p}{\partial z} + \varepsilon^2\frac{\partial^2 u}{\partial z^2} + \frac{1}{r}\frac{\partial}{\partial r}\Big(r\frac{\partial u}{\partial r}\Big), \tag{6a}$$

$$\varepsilon^3 \mathrm{Re}\Big(\frac{\partial v}{\partial t} + u\frac{\partial v}{\partial z} + v\frac{\partial v}{\partial r}\Big) = -\frac{\partial p}{\partial r} + \varepsilon^4\frac{\partial^2 v}{\partial z^2} + \varepsilon^2\frac{\partial}{\partial r}\Big(\frac{1}{r}\frac{\partial}{\partial r}\big(rv\big)\Big), \tag{6b}$$

$$\frac{\partial u}{\partial z} + \frac{1}{r}\frac{\partial}{\partial r}\big(rv\big) = 0, \tag{6c}$$

where $\mathrm{Re} = \rho VD/\eta$ is the Reynolds number.

According to [4, p.7], the velocity of the plunger, which can be used as a characteristic velocity, if the cross section of the annular channel compared to the plunger cross section is not too small[1], is typically $V = 10^{-1}$ m/s. A typical channel width is $D \approx 10^{-2}$m. A typical length of the plunger is 10^{-1} m. The dynamic viscosity of glass varies greatly with temperature, but for a temperature around 800 °C it is of the order of 10^4 kg/ms. The density

[1] as follows from an axial mass flux balance; see Section 6.1

of glass is 2500 kg/m^3 [5, p.4]. Therefore, we obtain typically $\varepsilon = \frac{1}{10}$, $\mathrm{Re} = 2{\cdot}5 \times 10^{-4}$, $\varepsilon\mathrm{Re} = 2{\cdot}5 \times 10^{-5}$, and $\varepsilon^3\mathrm{Re} = 2{\cdot}5 \times 10^{-7}$, and we can ignore the inertia and radial-friction terms to obtain

$$\frac{\partial p}{\partial z} = \frac{1}{r}\frac{\partial}{\partial r}\Big(r\frac{\partial u}{\partial r}\Big), \quad \frac{\partial p}{\partial r} = 0, \quad \frac{\partial u}{\partial z} + \frac{1}{r}\frac{\partial}{\partial r}(rv) = 0. \tag{7a, b, c}$$

with an assumed error of $O(\varepsilon^2)$ because $\mathrm{Re} < \varepsilon$. This set of equations may be recognized as Reynolds's lubrication-flow equations in cylindrical coordinates [6, p.83].

4. The temperature remains constant

Although in viscous flow the energy equation is decoupled from the equation of motion (4*a*), if the flow is incompressible and Newtonian with constant viscosity, the validity of this assumption is not obvious in the present problem. The viscosity is highly temperature-dependent, as is seen from the VFT (Vogel, Fulcher, Tamman)-relation [1, p.936]

$$\log_{10}\eta = A + \frac{B}{T - T_0},$$

where A, B, T_0 are constants depending on the glass composition (for example $A = -2.4$, $B = 4032$, and $T_0 = 170$ for Soda-Silica Glasses [7]), while T is in degrees Celsius. In this case $T = 800$ yields a viscosity of $\eta = 10^4$ kg/ms.

The high viscous forces may generate heat by friction, and the walls may supply or absorb heat by conduction, such that, with the temperature, the viscosity varies along the flow.

To investigate this possibility we will analyse the energy equation and estimate the order of magnitude of the various terms. The energy conservation law for viscous and compressible fluids may be written as [8, p.10]

$$\frac{\partial}{\partial t}(\rho e) + \nabla\cdot(\rho \boldsymbol{v} e) = -p\nabla\cdot\boldsymbol{v} - \nabla\cdot\boldsymbol{q} + \boldsymbol{\tau}:\nabla\boldsymbol{v}, \tag{8}$$

where e denotes the internal energy per unit of mass, $\boldsymbol{q}$ is the heat flux due to heat conduction, and $\boldsymbol{\tau}$ denotes the viscous stress tensor. Since we are only interested in an order-of-magnitude estimate, we assume $e \simeq c_p T$, where c_p is the heat capacity at constant pressure and T is the absolute temperature [9, p.31], and for $\boldsymbol{q}$ Fourier's law $\boldsymbol{q} = -k\nabla T$, where k is the heat conductivity.

In an incompressible flow with constant c_p and k we have

$$\rho c_p\Big(\frac{\partial T}{\partial t} + \boldsymbol{v}\cdot\nabla T\Big) = k\nabla^2 T + \eta(\dot{\boldsymbol{\gamma}}:\nabla\boldsymbol{v}).$$

We non-dimensionalize as before

$$r = Dr^*,\ z = Lz^*,\ v = \varepsilon V v^*,\ u = Vu^*,\ T = T_m + \Delta T\, T^*,\ \eta = \eta_g\eta^*,\ t = \frac{L}{V}t^*,$$

where $\Delta T = T_g - T_m$ and η_g denotes the glass viscosity at the bulk temperature. (Note that in the rest of the paper we use a constant viscosity $\eta = \eta_g$.) We find (ignoring the asterisks $*$)

$$\varepsilon\Big[\frac{\partial T}{\partial t} + \boldsymbol{v}\cdot\nabla T\Big] = \frac{1}{\mathrm{Pe}}\Big[\frac{1}{r}\frac{\partial}{\partial r}\Big(r\frac{\partial T}{\partial r}\Big) + \varepsilon^2\frac{\partial^2 T}{\partial z^2}\Big] + \frac{\mathrm{Ec}}{\mathrm{Re}}\eta\Big[\Big(\frac{\partial u}{\partial r} + \varepsilon^2\frac{\partial v}{\partial z}\Big)^2 + 2\varepsilon^2\Big(\Big[\frac{\partial v}{\partial r}\Big]^2 + \Big[\frac{v}{r}\Big]^2 + \Big[\frac{\partial u}{\partial z}\Big]^2\Big)\Big] \tag{9}$$

with Reynolds number $\mathrm{Re} = \rho V D/\eta_g$, Eckert number $\mathrm{Ec} = V^2/c_p\Delta T$, and Peclet number $\mathrm{Pe} = \rho V D c_p/k$. (Note that Pe and Re are related through the Prandtl number as $\mathrm{Pe} = \mathrm{RePr}$, while $\mathrm{PeEc/Re} = \mathrm{Br}$ is called the Brinkman number.) When we substitute the following values, typical of glass at 800 °C,

D : typical parison length scale	$= 10^{-2}$ m	T_g : glass temperature	= 800 °C,
V : typical plunger velocity	$= 10^{-1}$ m/s	T_m : mould temperature	= 500 °C,
ρ : glass density	$= 2500$ kg/m^3	c_p : glass heat capacity	= 1100 J/kg °C
η_g : glass dynamic viscosity	$= 10^4$ kg/ms	k : glass thermal conductivity	= 1.7 W/m °C
L : typical plunger length scale	$= 10^{-1}$ m		

we get the following dimensionless numbers:

$$\varepsilon = 10^{-1}, \quad \frac{1}{\mathrm{Pe}} = 6 \cdot 2 \times 10^{-4}, \qquad \frac{\mathrm{Ec}}{\mathrm{Re}} = 1 \cdot 2 \times 10^{-4}.$$

Both $1/(\varepsilon\mathrm{Pe})$ and $\mathrm{Ec}/(\varepsilon\mathrm{Re})$ are very small numbers, so in the bulk of the flow we can ignore the heat-conduction and thermal-production terms (the second and third term in Equation 9) against the convection (first) term. Hence, the energy equation simplifies to

$$\frac{\partial T}{\partial t} + \boldsymbol{v}\cdot\nabla T = \frac{\mathrm{d}T}{\mathrm{d}t} = 0,$$

indicating that the temperature is preserved following the flow. So, if we start with a uniform temperature field, it will remain uniform everywhere, and it follows that the viscosity also remains constant.

Note that this is not true in the thin temperature boundary layer along the wall, where the temperature varies from its value at the wall to the bulk temperature, and the conduction term is comparable with the convection term. From this balance,

$$\boldsymbol{v}\cdot\nabla T \sim \frac{1}{\varepsilon\mathrm{Pe}}\Big[\frac{\partial^2 T}{\partial r^2} + \frac{1}{r}\frac{\partial T}{\partial r}\Big],$$

it follows that the dimensionless boundary-layer thickness is of the order of $O((\varepsilon\mathrm{Pe})^{-1/3})$ (no slip) or $O((\varepsilon\mathrm{Pe})^{-1/2})$ (with slip). For the values considered this corresponds to boundary-layer thicknesses of, respectively, $\sim 2\times10^{-1}$ and $\sim 0{\cdot}8\times10^{-1}$, or 20% and 8% of the channel width. These values are, of course, not very small. However, to make progress we will for the moment consider them small enough to be ignored.

A small countereffect that may occur is that very close to the wall, where the glass temperature attains that of the wall, the viscosity increases by several orders of magnitude. For the present example the dimensionless viscosity is equal to $\eta(T_m) = 10^{5{\cdot}8}$, which leads to $(\mathrm{Ec}/\varepsilon\mathrm{Re})\eta(T_m) = 760$. So, with little or no slip between glass and wall (otherwise $\dot{\boldsymbol{\gamma}} : \nabla\boldsymbol{v}$ is small) the fluid friction is not negligible very close to the wall and will generate some heat. This may increase the temperature locally, and slightly counteract the lower wall temperature. The resulting decrease of viscosity could be called “self-lubrication”.

5. Boundary conditions

Depending on problem parameters such as wall temperature, fluid pressure, surface tension, or the presence of a lubricant like graphite powder [10, 11, 12, 13], the glass flow slips completely, partly or not at all along the wall. This means that the tangential component of the glass velocity $\boldsymbol{v}$ at the wall differs from the wall velocity $\boldsymbol{v}_w$, the difference being called the slip velocity. Since by assumption the glass flows in the (r, z)-plane and the plunger moves in the z-direction, it is sufficient to consider the tangential component in the (r, z)-plane.

Two slip conditions are commonly used. One is based on Coulomb friction [13], which is the assumption of a linear relation between tangential (shear) stress and normal stress (pressure), usually with a threshold value. The other is Navier's slip condition [6, p.87], which assumes a linear relation between the slip velocity and the shear stress. Physically, little is known as to which condition is essentially more correct. Therefore, we will take here Navier's slip condition, as it is mathematically more convenient here, since in our theory the pressure is only available as an integral, while the velocities are explicitly known.

The shear stress (Equations 2,3) applied to a surface with unit normal vector $\boldsymbol{n}$, defined as pointing *out* of the fluid, in the tangential direction $\boldsymbol{t}$, is given by $-(\boldsymbol{\sigma}\cdot\boldsymbol{n})\cdot\boldsymbol{t} = -(\boldsymbol{\tau}\cdot\boldsymbol{n})\cdot\boldsymbol{t}$. The slip velocity $(\boldsymbol{v} - \boldsymbol{v}_w)\cdot\boldsymbol{t}$ will be proportional to this stress in the (r, z)-plane

$$(\boldsymbol{v} - \boldsymbol{v}_w)\cdot\boldsymbol{t} = -s(\boldsymbol{\tau}\cdot\boldsymbol{n})\cdot\boldsymbol{t}\ , \tag{10}$$

where the slip factor s (a positive number) measures the amount of slip. (A better measure is the dimensionless version of s; see below.) There is no slip if $s = 0$, while there is no friction if $s = \infty$. The inverse, s^{-1}, might be called the friction factor. In general, s may be a function of position.

More advanced slip modelling, for example a nonlinear relation with s depending on pressure, is formally included in this way, if we in some way iteratively adapt s and the corresponding solution. We haven't investigated this possibility here, however.

For reference purposes, we note that, in cylindrical coordinates, the components of $\boldsymbol{\sigma}$ are given by

$$\begin{aligned}
\sigma_{rr} &= -p + 2\eta\frac{\partial v}{\partial r}, \quad \sigma_{\theta r} = \sigma_{r\theta} = 0, & \sigma_{\theta\theta} &= -p + 2\eta\frac{v}{r},\\
\sigma_{zz} &= -p + 2\eta\frac{\partial u}{\partial z}, \quad \sigma_{zr} = \sigma_{rz} = \eta\Big(\frac{\partial v}{\partial z} + \frac{\partial u}{\partial r}\Big), & \sigma_{\theta z} &= \sigma_{z\theta} = 0.
\end{aligned}$$

5.1. Boundary conditions on the plunger

To apply the above conditions to the moving plunger surface, we recall that this is defined as:

$$r = R_p(z - z_p(t)),$$

where $z = z_p(t)$ is the position of the top of the plunger at time t. Subscript "$_p$" denotes the value at the plunger. Unless indicated otherwise, we will write here $R_p = R_p(z - z_p)$.

The unit outward normal $\boldsymbol{n}_p$ and the counterclockwise-directed unit tangent $\boldsymbol{t}_p$ in the (r, z)-plane are given by

$$\boldsymbol{n}_p = \frac{R'_p\boldsymbol{e}_z - \boldsymbol{e}_r}{\sqrt{1 + R'^2_p}}, \qquad \boldsymbol{t}_p = \frac{-\boldsymbol{e}_z - R'_p\boldsymbol{e}_r}{\sqrt{1 + R'^2_p}}. \tag{11}$$

From the definition of stress (2, 3) we have

$$(\boldsymbol{\sigma}\cdot\boldsymbol{n}_p)\cdot\boldsymbol{t}_p = \eta\,\frac{(1-R_p'^2)\Big(\dfrac{\partial u}{\partial r}+\dfrac{\partial v}{\partial z}\Big)-2R_p'\Big(\dfrac{\partial u}{\partial z}-\dfrac{\partial v}{\partial r}\Big)}{1+R_p'^2}. \tag{12}$$

To determine the slip velocity, we note that the plunger is moving down with speed $\frac{\mathrm{d}z_p}{\mathrm{d}t} = u_p$. Thus, the (dimensional) slip velocity at the plunger surface is

$$(\boldsymbol{v}-u_p\boldsymbol{e}_z)\cdot\boldsymbol{t}_p = ((u-u_p)\boldsymbol{e}_z+v\boldsymbol{e}_r)\cdot\frac{-\boldsymbol{e}_z-R_p'\boldsymbol{e}_r}{\sqrt{1+R_p'^2}} = -\frac{(u-u_p)+vR_p'}{\sqrt{1+R_p'^2}}. \tag{13}$$

From Equations (10, 11, 13), we obtain the boundary condition on the plunger

$$\frac{(u-u_p)+vR_p'}{\sqrt{1+R_p'^2}} = s_p\eta\,\frac{(1-R_p'^2)\Big(\dfrac{\partial u}{\partial r}+\dfrac{\partial v}{\partial z}\Big)-2R_p'\Big(\dfrac{\partial u}{\partial z}-\dfrac{\partial v}{\partial r}\Big)}{1+R_p'^2}, \tag{14}$$

where s_p is s at the plunger. The other boundary condition at the plunger follows from the observation that the wall is solid, so $\boldsymbol{v}\cdot\boldsymbol{n} = 0$ or

$$v = (u-u_p)R_p'. \tag{15}$$

After introducing the following scaled slip coefficient s^*

$$s = \frac{D}{\eta}s^* \tag{16}$$

and using the same scaling as before, we obtain the dimensionless form of Equation (14) and (15) (with asterisks ignored),

$$\frac{(u-u_p)+\varepsilon^2vR_p'}{\sqrt{1+\varepsilon^2R_p'^2}} = s_p\,\frac{(1-\varepsilon^2R_p'^2)\Big(\dfrac{\partial u}{\partial r}+\varepsilon^2\dfrac{\partial v}{\partial z}\Big)-2\varepsilon^2R_p'\Big(\dfrac{\partial u}{\partial z}-\dfrac{\partial v}{\partial r}\Big)}{1+\varepsilon^2R_p'^2}, \tag{17}$$

$$v = (u-u_p)R_p'. \tag{18}$$

As the wall temperature or the amount of lubricant may vary along the wall, it is practically important to let s be a function of position. The present solution is perfectly valid for any varying slip factor, as long as axial symmetry is preserved, and s is a smooth function of position z:

$$s = s(z). \tag{19}$$

For small ε we obtain (with an error $O(\varepsilon^2)$) for the boundary condition (17)

$$u-u_p = s_p\frac{\partial u}{\partial r} \qquad \text{at } r = R_p, \tag{20}$$

where s_p, if non-constant, is to be interpreted as a property of the moving surface and therefore to be read as $s_p = s_p(z - z_p)$.

The other boundary condition (18) will be left as it is.

5.2. Boundary conditions on the mould

The surface of the mould, given by

$$r = R_m(z),$$

(subscript "$_m$" denotes the value at the mould) has unit outward normal $\boldsymbol{n}_m$ and counterclockwise-directed unit tangent $\boldsymbol{t}_m$ given by

$$\boldsymbol{n}_m = \frac{-R'_m \boldsymbol{e}_z + \boldsymbol{e}_r}{\sqrt{1 + R'^2_m}}, \qquad \boldsymbol{t}_m = \frac{\boldsymbol{e}_z + R'_m \boldsymbol{e}_r}{\sqrt{1 + R'^2_m}}. \tag{21}$$

In a similar way as for the boundary conditions on the plunger, we obtain the boundary condition on the mould as

$$\frac{u + v R'_m}{\sqrt{1 + R'^2_m}} = -s_m \eta \, \frac{(1 - R'^2_m)\left(\dfrac{\partial u}{\partial r} + \dfrac{\partial v}{\partial z}\right) - 2R'_m\left(\dfrac{\partial u}{\partial z} - \dfrac{\partial v}{\partial r}\right)}{1 + R'^2_m}, \tag{22}$$

and

$$v = u R'_m. \tag{23}$$

In dimensionless form the relations are,

$$\frac{u + \varepsilon^2 v R'_m}{\sqrt{1 + \varepsilon^2 R'^2_m}} = -s_m \, \frac{(1 - \varepsilon^2 R'^2_m)\left(\dfrac{\partial u}{\partial r} + \varepsilon^2 \dfrac{\partial v}{\partial z}\right) - 2\varepsilon^2 R'_m\left(\dfrac{\partial u}{\partial z} - \dfrac{\partial v}{\partial r}\right)}{1 + \varepsilon^2 R'^2_m}, \tag{24}$$

and

$$v = u R'_m, \tag{25}$$

Similarly, for small ε, boundary condition (24) becomes

$$u = -s_m \frac{\partial u}{\partial r} \qquad \text{at } r = R_m. \tag{26}$$

The other condition (25) will be left as it is.

5.3. The free surface

As the blob of glass does not initially fill the mould completely (see Figure 1), there is a free surface of glass moving into the annular duct between mould and plunger. At the free boundary, the normal stress must be equal to external pressure p_0, which is assumed to be constant

$$(\boldsymbol{\sigma} \cdot \boldsymbol{n}) \cdot \boldsymbol{n} = p_0,$$

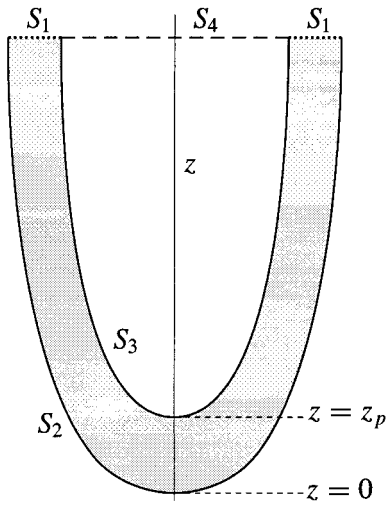

Figure 4. Sketch of the control surfaces to calculate the flux.

and the tangential stress must be equal to zero

$$(\boldsymbol{\sigma}\cdot\boldsymbol{n})\cdot\boldsymbol{t} = 0.$$

In our slender-geometry approximation the exact shape of the free surface cannot be determined. In its neighbourhood the flow scales both in the r and z directions on the thickness D of the annular channel. In other words, the flow is no longer slowly varying in z, rendering the present approximation invalid.

Within the present approximation (and assumption of circular symmetry), we will deal with the average level b of the free surface as follows (in scaled variables):

$$p = 0 \qquad \text{at } z = b(t), \tag{27}$$

where b is a function of the time-dependent geometry, implicitly defined in such a way that the (incompressible) glass volume between $z = 0$ and $z = b(t)$ is constant for all t.

6. Some auxiliary results

In this section, we derive some expressions (to be used later) for the axial flux and the total force on the plunger.

6.1. THE FLUX

Consider the flux at some level z through cross section S_1 (see Figure 4). The value of this flux depends on z, since the plunger moves downwards and causes the glass to move upwards through a varying cross section. We will use this value later to find the pressure gradient.

Since glass is an incompressible fluid, we have from Gauss's divergence theorem

$$0 = \int_\Omega \nabla\cdot\boldsymbol{v}\,\mathrm{d}\boldsymbol{x} = \int_{\partial\Omega} \boldsymbol{v}\cdot\boldsymbol{n}\,\mathrm{d}S = \int_{S_1} \boldsymbol{v}\cdot\boldsymbol{n}\,\mathrm{d}S + \int_{S_2} \boldsymbol{v}\cdot\boldsymbol{n}\,\mathrm{d}S + \int_{S_3} \boldsymbol{v}\cdot\boldsymbol{n}\,\mathrm{d}S \tag{28}$$

where $\boldsymbol{v} = u\boldsymbol{e}_z + \varepsilon v\boldsymbol{e}_r$. Since the mould is stationary and impermeable, we have

$$\int_{S_2} \boldsymbol{v}\cdot\boldsymbol{n}\,\mathrm{d}S = 0,$$

while the flux through S_1 is given by

$$\int_{S_1} \boldsymbol{v}\cdot\boldsymbol{n}\,\mathrm{d}S = 2\pi\int_{R_p}^{R_m} ru(r,z)\,\mathrm{d}r\ .$$

To calculate $\int_{S_3}\boldsymbol{v}\cdot\boldsymbol{n}\,\mathrm{d}S$, we note that it would make no difference for the amount of glass displaced by the plunger if the plunger were filled with glass, because glass is just as incompressible as the solid plunger. Therefore, instead of control surface S_3, we might as well use surface S_4, which yields more easily the result

$$\int_{S_3} \boldsymbol{v}\cdot\boldsymbol{n}\,\mathrm{d}S = \int_{S_4} \boldsymbol{v}\cdot\boldsymbol{n}\,\mathrm{d}S = \pi u_p R_p^2\ .$$

It follows that the flux is given by

$$2\pi\int_{R_p}^{R_m} ru(r,z)\,\mathrm{d}r = -\pi u_p R_p^2\ . \tag{29}$$

6.2. The total force on the plunger

In this section we discuss the total force on the plunger and use the result to find the velocity of the plunger. We return for a moment to a dimensional formulation. Later, we will turn to the dimensionless formulation.

The force (= stress×surface) in direction $\boldsymbol{e}_k$, applied to an infinitesimal surface element $\mathrm{d}S$ with outward normal $\boldsymbol{n}$, is by definition

$$-(\boldsymbol{\sigma}\cdot\boldsymbol{n})\cdot\boldsymbol{e}_k\,\mathrm{d}S = -\sum_j \sigma_{kj}n_j\,\mathrm{d}S.$$

At the plunger surface with unit normal $\boldsymbol{n}_p$, given in (11), the stress in the z-direction is

$$-(\boldsymbol{\sigma}\cdot\boldsymbol{n}_p)\cdot\boldsymbol{e}_z = \left\{\Big(p - 2\eta\frac{\partial u}{\partial z}\Big)R_p' + \eta\Big(\frac{\partial v}{\partial z} + \frac{\partial u}{\partial r}\Big)\right\}\frac{1}{\sqrt{1+R_p'^{\,2}}},$$

where $R_p = R_p(z - z_p(t))$.

A (circular) surface element is given by

$$\mathrm{d}S = 2\pi R_p\sqrt{1+R_p'^{\,2}}\,\mathrm{d}z.$$

Thus, the total force on the plunger between top level $z = z_p(t)$ and glass level $z = b(t)$ is given by

$$f = 2\pi\int_{z_p}^{b}\left[\Big(p - 2\eta\frac{\partial u}{\partial z}\Big)R_p' + \eta\Big(\frac{\partial v}{\partial z} + \frac{\partial u}{\partial r}\Big)\right]_{r=R_p} R_p\,\mathrm{d}z. \tag{30}$$

Note that this glass level, as a function of time, is yet to be determined (see next section).

We render Equation (30) dimensionless by using the same scaling as before, with $b = Lb^*$, and scale the force as

$$f = 2\pi\eta V L f^*.$$

This yields (ignoring again the asterisks) :

$$f = \int_{z_p}^{b} \left[\left(p - 2\varepsilon^2 \frac{\partial u}{\partial z} \right) R_p' + \varepsilon^2 \frac{\partial v}{\partial z} + \frac{\partial u}{\partial r} \right]_{r=R_p} R_p \, \mathrm{d}z \simeq \int_{z_p}^{b} \left[p R_p' + \frac{\partial u}{\partial r} \right]_{r=R_p} R_p \, \mathrm{d}z. \tag{31}$$

7. Results

7.1. The velocity and pressure fields

Now we are ready to solve the Equations (**??***a-c*) with boundary conditions (20,18) and (26,25). First we note that p is a function of z only. Then Equation (**??***a*)

$$\frac{\mathrm{d}p}{\mathrm{d}z} = \frac{\partial^2 u}{\partial r^2} + \frac{1}{r}\frac{\partial u}{\partial r} = \frac{1}{r}\frac{\partial}{\partial r}\left(r \frac{\partial u}{\partial r} \right)$$

has solution

$$u = \frac{1}{4} r^2 \frac{\mathrm{d}p}{\mathrm{d}z} + A(z) \ln(r) + B(z).$$

Using boundary conditions (20) and (26), we obtain:

$$u = \frac{1}{4}\frac{\mathrm{d}p}{\mathrm{d}z}\left[r^2 + \frac{\beta_m(\alpha_p - \log r) - \beta_p(\alpha_m - \log r)}{\alpha_m - \alpha_p} \right] + u_p \, \frac{\alpha_m - \log r}{\alpha_m - \alpha_p}, \tag{32}$$

where it has been found convenient to introduce auxiliary parameters $\alpha_{p,m}$, $\beta_{p,m}$ and $\gamma_{p,m}$ as follows

$$\sigma_m = s_m / R_m, \;\; \sigma_p = -s_p / R_p, \;\; \alpha = \log R + \sigma, \;\; \beta = R^2(1 + 2\sigma), \;\; \gamma = R^4(1 + 4\sigma), \tag{33}$$

showing at the same time the curious result that the essential slip parameter in a duct is apparently not s itself, but the product of s and the wall curvature.

Using Equation (32), the expression for u (29), the relation for the flux, and the following integral for ru

$$\int ru(r,z)\,\mathrm{d}r = \tfrac{1}{8} r^2 \frac{\mathrm{d}p}{\mathrm{d}z} \left[\tfrac{1}{2} r^2 + \frac{\beta_m(\alpha_p + \frac{1}{2} - \log r) - \beta_p(\alpha_m + \frac{1}{2} - \log r)}{\alpha_m - \alpha_p} \right] + \ldots$$
$$+ \tfrac{1}{2} r^2 u_p \, \frac{\alpha_m + \frac{1}{2} - \log r}{\alpha_m - \alpha_p}, \tag{34}$$

we can determine the pressure gradient to find

$$\frac{\mathrm{d}p}{\mathrm{d}z} = -4u_p \frac{\beta_m - \beta_p}{(\beta_m - \beta_p)^2 - (\alpha_m - \alpha_p)(\gamma_m - \gamma_p)} \tag{35}$$

leading with Equation (27) to

$$p(z) = -\int_z^b \frac{\mathrm{d}p}{\mathrm{d}z}\,\mathrm{d}z\ . \tag{36}$$

Finally we solve Equation (**??***c*) with boundary conditions (18) or (25). (Only one will be needed, as the other has already been used implicitly when we determined the axial flux). We can rewrite Equation (**??***c*) as

$$\frac{\partial}{\partial r}(vr) + r\frac{\partial u}{\partial z} = 0,$$

and then use (25), to obtain

$$v = \frac{A(z)}{r} - \frac{1}{r}\int r\frac{\partial u}{\partial z}\,\mathrm{d}r = \frac{1}{r}\Big(R_m R_m' u(R_m, z) + \int_r^{R_m} r\frac{\partial u}{\partial z}\,\mathrm{d}r\Big) = \frac{1}{r}\frac{\mathrm{d}}{\mathrm{d}z}\int_r^{R_m} ru(r, z)\,\mathrm{d}r. \tag{37}$$

Upon substituting (34) in (37) and subsequent differentiation, we obtain (a complicated expression for) v (see appendix). It may be verified that boundary condition (18) indeed is satisfied.

7.2. The force on the plunger

By substituting the above results in Equation (31), we obtain to leading order

$$\begin{aligned} f &= \int_{z_p}^b \Big(p\frac{\mathrm{d}R_p}{\mathrm{d}z} + \Big[\frac{\partial u}{\partial r}\Big]_{r=R_p}\Big)R_p\,\mathrm{d}z = \int_{z_p}^b \Big(-\tfrac{1}{2}R_p^2\frac{\mathrm{d}p}{\mathrm{d}z} + \Big[\frac{\partial u}{\partial r}\Big]_{r=R_p} R_p\Big)\,\mathrm{d}z = \\ &= u_p\int_{z_p}^b \frac{\gamma_m - \gamma_p}{(\beta_m - \beta_p)^2 - (\alpha_m - \alpha_p)(\gamma_m - \gamma_p)}\,\mathrm{d}z. \end{aligned} \tag{38}$$

Although the approximation is strictly speaking no longer valid at $z = z_p$, the integral converges, and the contribution of the plunger-tip area does seem to be asymptotically of lower order.

An interesting conserved quantity of the process is the time integral of the plunger force. (Dimensionally equivalent to a net change of momentum, although inertia plays no rôle in the present model.) It only depends on the end points z_1 and z_2 and not on the way the plunger moves in time, because f depends linearly on u_p.

$$\int_{t_1}^{t_2} f(t)\,\mathrm{d}t = \int_{z_1}^{z_2}\int_{z_p}^b \frac{\gamma_m - \gamma_p}{(\beta_m - \beta_p)^2 - (\alpha_m - \alpha_p)(\gamma_m - \gamma_p)}\,\mathrm{d}z\,\mathrm{d}z_p\ . \tag{39}$$

This is not a unique property of the approximation, but a direct consequence of the fact that in the Stokes equations time is only a parameter, so that velocities may be scaled on u_p, and the plunger force f on $\eta u_p z_p$.

7.3. A PRESCRIBED FORCE OR VELOCITY OF THE PLUNGER

In this section, we consider the relation between time and velocity of the plunger, assuming the velocity of, or the force on the plunger to be a prescribed function of t and the total volume of the glass is constant.

During the pressing phase, the plunger moves downwards as the glass moves upwards. So the plunger velocity u_p or the total force f, the position of the top of the plunger z_p, and the glass level b vary with time. Therefore we have to find a system of three equations for z_p, b, and u_p or f.

First, we observe that for all t the (scaled) volume Ω of the total amount of glass is equal to the constant

$$\Omega = \pi \int_0^b R_m^2 \,\mathrm{d}z - \pi \int_{z_p}^b R_p^2 \,\mathrm{d}z. \tag{40}$$

So, if we could solve this equation explicitly, we would have a functional relationship between b and z_p. This, however, is only possible in the simplest cases, for example when both R_p and R_m are parabolas. In general it has to be solved numerically for each time step. A natural approach is therefore to rewrite this equation as a differential equation in time that can be solved by standard numerical integration routines.

After differentiating Equation (40), using the defining relation between z_p and u_p and the relation (38) between f and u_p, we obtain the following system of equations

$$\frac{\mathrm{d}z_p}{\mathrm{d}t} = u_p. \tag{41a}$$

$$\frac{\mathrm{d}b}{\mathrm{d}t} = -u_p \left.\frac{R_p^2}{R_m^2 - R_p^2}\right|_{z=b}. \tag{41b}$$

$$f = u_p \int_{z_p}^b G(z, z_p)\,\mathrm{d}z, \quad G(z, z_p) = \frac{\gamma_m - \gamma_p}{(\beta_m - \beta_p)^2 - (\alpha_m - \alpha_p)(\gamma_m - \gamma_p)}. \tag{41c}$$

which can be integrated numerically with either $f(t)$ or $u_p(t)$ given. In the simpler case when u_p is given, Equation (41*c*) only defines f and is decoupled from the others.

8. Examples

In this section we present two examples. In the first we compare the present analytic expressions for u and εv with numerical results obtained from a numerical model for glass flow as developed by the TUE Scientific Computing Group of Professor R.M.M. Mattheij. We use here simple parabolic profiles for the plunger and mould, and the plots are in terms of non-dimensional quantities.

In the second example we consider the velocity of the plunger as it results from a given force. In addition, we use a practically more representative geometry of plunger and mould, as given in Figure 7*b*. The plots are expressed in dimensional quantities.

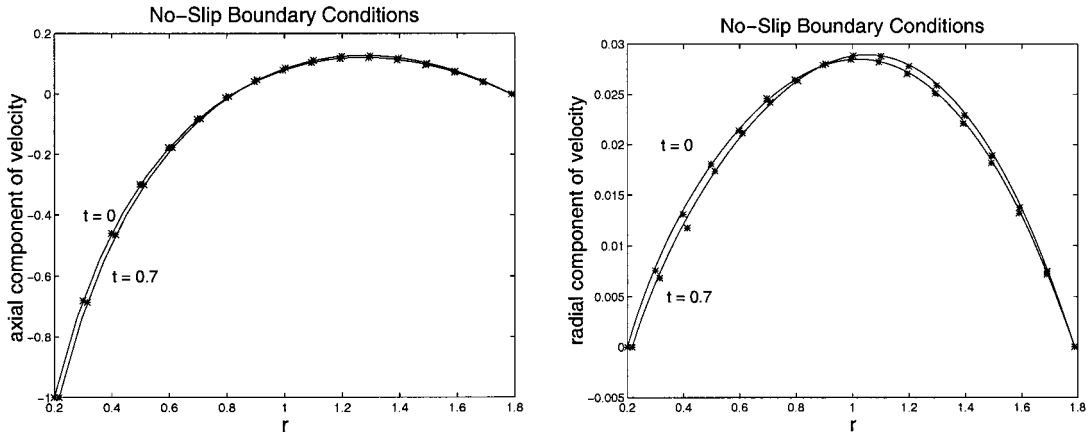

a. Axial velocity u *b.* Radial velocity εv

Figure 5. Axial and radial velocity. Parabolic geometry, no-slip. (Dimensionless.)

8.1. A GIVEN PLUNGER VELOCITY

Define the geometries and motion of plunger and mould by the following (dimensionless) expressions

$$R_p(z) = 0{\cdot}1\sqrt{5}\sqrt{z}, \quad R_m(z) = 0{\cdot}8\sqrt{5}\sqrt{z}, \quad z_p(t) = 1 - t,$$

where $\varepsilon = \frac{1}{5}$ and $u_p = -1$, while we will consider $z = 1$. Two cases are considered: (i) with no-slip boundary conditions ($s_p = s_m = 0$) and (ii) with mixed boundary conditions ($s_p = \infty$ and $s_m = 0$). The results will be presented in dimensionless form, although for a proper comparison the velocities will be scaled both on the same (plunger) velocity. In other words, in the figures the axial velocity u and radial velocity εv are plotted.

In Figure 5 we have case (i). Note that the order of magnitude of the axial velocity u is indeed the same as that of the plunger (dimensionless unity), because of the no-slip condition at both sides. It is seen that there is an exceptionally good agreement between the numerical ($*$) and the analytic solution (solid line).

Next we consider case (ii), with mixed boundary conditions. By taking $s_p \to \infty$ in Equation (20), we obtain $\frac{\partial u}{\partial r} = 0$. Next, we have of course Equation (18). On the stationary mould there is no slip, so here we have simply the boundary condition $u = v = 0$. As there is complete slip at the plunger wall, the velocity of the plunger plays no direct role in the problem. The axial velocity is now determined by the effect of plunger displacement. As a result, the order of magnitude of u is considerably lower than unity. The results of this case are presented in Figure 6. In the axial velocity (Figure 6*a*) the numerical solution ($*$) appears to differ a little from the analytical solution (solid line). This is, however, exactly consistent with the (conjectured) error of the asymptotic approximation, which is $O(\varepsilon^2) \sim 4\%$. Since $s_p = \infty$, Equation (10) becomes $(\boldsymbol{\sigma} \cdot \boldsymbol{n}) \cdot \boldsymbol{t} = 0$ at the plunger. For small ε this reduces to the approximate value $\frac{\partial u}{\partial r} = 0 + O(\varepsilon^2)$. This is different from the no-slip case where the condition $u = 0$ is not only satisfied approximately but exactly.

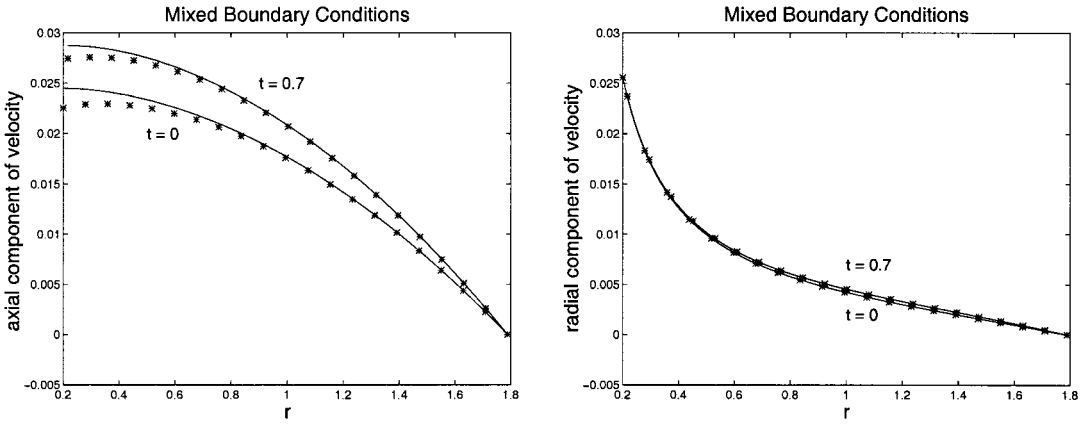

a. Axial velocity u *b*. Radial velocity εv

Figure 6. Axial and radial velocity. Parabolic geometry, mixed slip. (Dimensionless.)

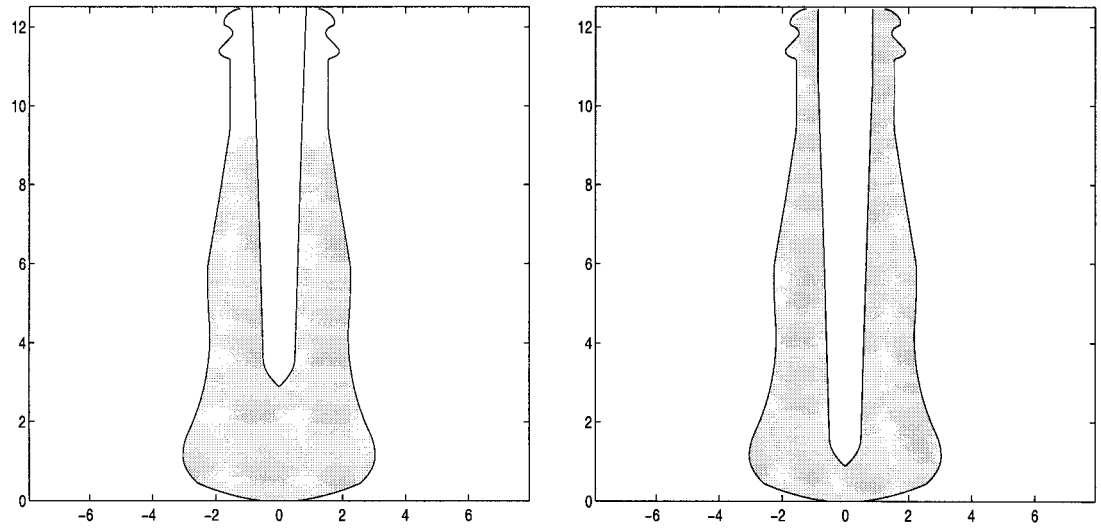

a. Plunger is going down *b*. Plunger in end position

Figure 7. Realistic geometry of parison (units: cm)

8.2. A GIVEN PLUNGER FORCE

In this example we consider a more realistic situation. We will take a geometry of a real parison (Figure 7*b*), and we will apply a given force from which the plunger velocity results, using the results of Sections 7.2 and 7.3, all in dimensional units. As in example 1, we use two types of boundary condition: no slip ($s_p = s_m = 0$) and mixed ($s_p = \infty$ and $s_m = 0$). The force on the plunger will be assumed constant. Figure 7*b* shows the final position of the plunger in the pressing phase. In order to make the calculation easier, we calculated backwards in time, starting with this final position at $t = 0$. Since the Stokes equations do not include inertial effects, the sign of the time is irrelevant and the results of a forward and a backward calculation are exactly the same. The problem parameters, related to these cases, are the same as given in the table of section 4, namely: $V = 10\,\text{cm/s}$, $D = 1\,\text{cm}$, $\eta = 10^4\,\text{kg/(s m)}$, $\varepsilon = 0{\cdot}1$

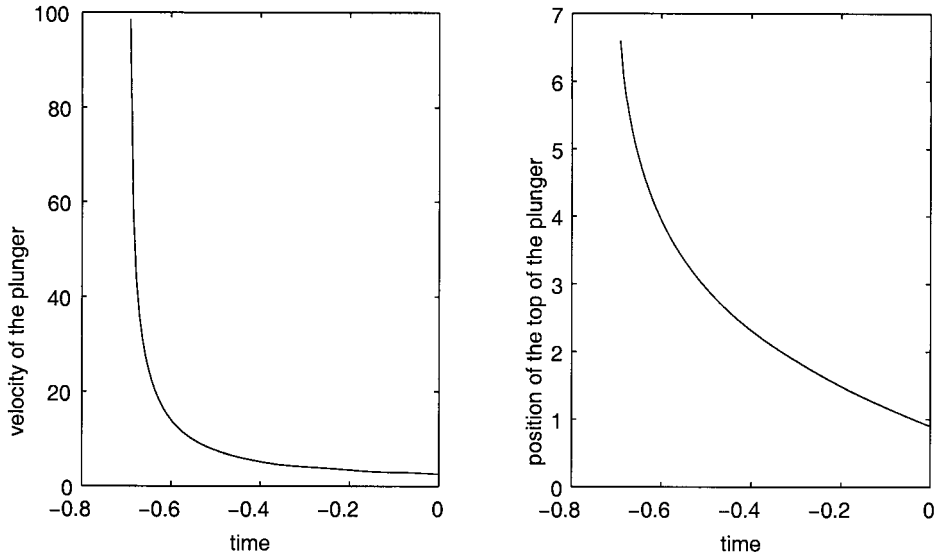

Figure 8. Given force = 7500 N, and $s_p = s_m = 0$ (units: sec and cm/s).

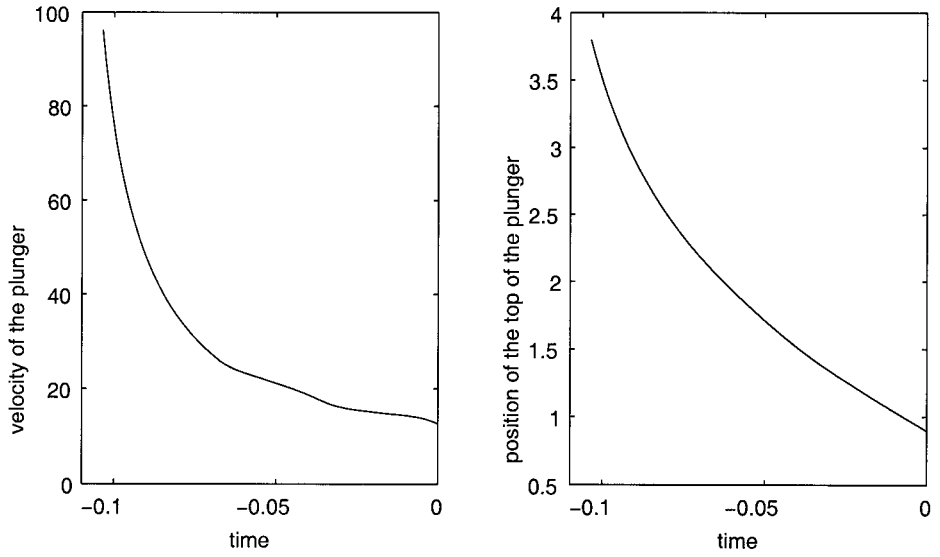

Figure 9. Given force = 5000 N, $s_p = \infty$, and $s_m = 0$ (units: sec and cm/s).

and $z = 1$. This suggests that the results are typically correct with an error of the order of 1%. In the case of Figure 8 (without slip) the applied plunger force is $f = 7500\,\mathrm{N}$, while in the case of Figure 9 (with slip) the force is $f = 5000\,\mathrm{N}$.

Evidently, when we go further back in time until the very early splash of the plunger in the fluid, and assume that the plunger force is still the same, the absence of resistence leads to unlimited high velocities. This, however, is impossible in practice, as the power ($\sim$ force $\times$ velocity) of the equipment is limited, and the inertia of the plunger is nonzero.

8.3. Numerical Method

A detailed description of the numerical method used in example 1 may be found in [14, p.209]. In summary, it is described as follows: the glass flow is modelled by the Stokes equations, *i.e.*, for vanishing Reynolds number. The (self-adaptive) discretization scheme of the domain is based on a triangular mesh, where each triangle has twelve degrees of freedom for the velocity components. On each triangle the pressure is constant and the velocity is piecewise linear. The Finite-Element Method (second order with respect to the size of mesh) is used to solve the Stokes equations, with an indicated accuracy of at least three digits. The time evolution of the glass domain Ω is found by solving the ordinary differential equation

$$\frac{\mathrm{d}\mathbf{x}(t)}{\mathrm{d}t} = \mathbf{v}(\mathbf{x}(t)),\ t \in [t_n, t_{n+1}], \tag{42a}$$

$$\mathbf{x}(t_n) \in \Omega_{t_n}. \tag{42b}$$

9. Conclusions

We have described a model for highly viscous incompressible glass flow during the pressing phase of the production. The model includes a general slip boundary condition. By using a perturbation method based on the slender geometry and low Reynolds number, we obtained explicit expressions for flow velocity and pressure gradient.

Based on these results, we calculated the total force on the plunger for given plunger velocity, and an ordinary differential equation for the resulting plunger velocity when the force is prescribed.

Representative examples showed a very good agreement of the flow velocity between the present solution and numerically obtained "exact" FEM solutions. We conclude that the perturbation method based on the slender geometry is an appropriate approach to this problem.

Appendix : $v(r, z)$

In this appendix, we derive the expression for $v(r, z)$. We already got (Equation 37)

$$v = \frac{1}{r}\frac{\mathrm{d}}{\mathrm{d}z}\int_r^{R_m} r u(r, z)\mathrm{d}r. \tag{A1}$$

Using Equations (34) and (35), we obtain

$$\begin{aligned}\int_r^{R_m} r u(r, z)\,\mathrm{d}r = \frac{u_p}{4}\left(\frac{\beta_m - \beta_p}{\alpha_m - \alpha_p}\right)\Big\{&(R_m^4 - r^4)(\alpha_m - \alpha_p)\ldots\\ &+2(\beta_m - \beta_p)r^2\log\left(\tfrac{r}{R_p}\right) - 2(\beta_m R_m^2 - \beta_p r^2)\log\left(\tfrac{R_m}{R_p}\right) + \frac{\beta_m\beta_p(R_m^2 - R_p^2)(R_m^2 - r^2)}{R_m^2 R_p^2}\Big\}\times\ldots\\ &\left\{(R_m^4 - R_p^4)(\alpha_m - \alpha_p) - 2(\beta_m R_m^2 - \beta_p R_p^2)\log\left(\tfrac{R_m}{R_p}\right) + \beta_m\beta_p\left(\frac{R_m}{R_p} - \frac{R_p}{R_m}\right)^2\right\}^{-1}\ldots\\ &- \frac{u_p}{4}\left[\frac{\beta_m(1 - \frac{r^2}{R_m^2}) + 2r^2\log\left(\frac{R_m}{r}\right)}{\alpha_m - \alpha_p}\right].\end{aligned} \tag{A2}$$

From Equation (33), we obtain for the z-derivatives of $\alpha_{m,p}$ and $\beta_{m,p}$

$$\alpha' = \frac{R'}{R}(1-\sigma) \pm \frac{s'}{R}, \qquad \beta' = 2RR'(1+\sigma) \pm 2Rs'. \tag{A3}$$

By differentiating Equation (A2) with respect to z and using Equations (A3), we obtain the full expression of v.

Acknowledgements

We are grateful for the cooperation with the TUE Scientific Computing Group of Professor R.M.M. Mattheij, who generously provided the results from the numerical glass-flow simulation. In particular, we want to express our gratitude to Bram van de Broek and L.G.F.C. van Bree. We are grateful for the helpfull discussions with Dr J.K.M. Jansen, Dr Y. Knops, and K. Laevsky. Especially appreciated are the many suggestions and fruitful ideas from Dr Peter Howell. Finally, we are grateful to the referees for their very constructive remarks.

References

1. F.V. Tooley, *The Handbook of Glass Manufacture Vol II*. New York: Books For Industry, Inc, and Glass Industry Magazine (1974) 1147pp.
2. Ph. Simons and R.M.M. Mattheij, *The Cooling of Molten Glass In a Mould*. Rana 95-21, Eindhoven University of Technology (1995) 10pp.
3. J. Kevorkian and J.D. Cole, *Multiple Scale and Singular Perturbation Methods*. New-York: Springer-Verlag (1996) 632pp.
4. W.A. van den Broek, *Glass Morphology in Manufacturing Jars*. Master's Thesis. Eindhoven University of Technology (1996) 77pp.
5. S.L. de Snoo, R.M.M. Mattheij, and G.A.L. van de Vorst, *Modelling of Glass, in Particular Small Scale Surface Changes*. Rana 96-11, Eindhoven University of Technology (1996) 21pp.
6. A.C. Fowler, *Mathematical Models in the Applied Sciences*. Cambridge: Cambridge University Press (1998) 402pp.
7. C.L. Babcock, Viscosity and electrical conductivity of molten glasses. *J. Amer. Ceramic Soc.* 17 (1934) 329–342.
8. L.D. Landau and E.M. Lifshitz, *Fluid Mechanics* (2nd ed.). Oxford: Pergamon (1987) 539pp.
9. Y. Yener and S. Kakac, *Heat Conduction* (3rd ed.). Washington, DC: Taylor & Francis (1993) 363pp.
10. W.C. Dowling, H.V. Fairbanks, and W.A. Koehler. A study of the effect of lubricants on molten glass to heated metals. *J. Amer. Ceramic Soc.* 33 (1950) 269–273.
11. W. Trier, and F. Hassoun, Mechanik des Gleitens heißen, zähflüssigen Glases auf Metalloberflächen. *Glastechnische Berichte* 45 (1972) 271–276.
12. W. Trier, Gleitverhalten von heißem, zähflüssigem Glas auf Metalloberflächen. *Glastechnische Berichte* 51 (1978) 240–243.
13. M. Falipou, F. Sicloroff, and C. Donnet, New method for measuring the friction between hot viscous glass and metals. *Glastechnische Berichte* 72 (1999) pp.59–66.
14. K. Laevsky and R.M.M. Mattheij, Mathematical modeling of some glass problems. In: A. FASANO (ed.), *Complex Flows in Industrial Processes.* Boston: Birkhäuser Boston (2000) pp.191–214.